

# Investigation of chalcopyrite film growth: an evolution of thin film morphology and structure during selenization

Jun-feng Han · Cheng Liao · Tao Jiang ·  
Hua-mu Xie

Received: 15 June 2013 / Accepted: 18 August 2013 / Published online: 25 August 2013  
© Springer Science+Business Media New York 2013

**Abstract** In this work, we report a study of the evolution of Cu–In–Ga–Se system during selenization. The metallic precursors were selenized in Se vapour atmosphere at temperature range from 210 to 380 °C. Scanning electron microscopy, transmission electron microscopy, X-ray diffraction, Raman spectra were used to investigate morphological and structural properties of the films. A great amount of thin platelets appeared in the film surfaces at temperature range from 210 to 270 °C. Most platelets had hexagon or polygon structures. The average sizes of these platelets increased with the temperatures. TEM analyses indicated that these platelets had  $\gamma$ -CuSe phases. Beyond 310 °C, most of CuSe platelets decomposed under release of selenium and formed  $\text{Cu}_{2-x}\text{Se}$ .  $\text{Cu}_{2-x}\text{Se}$  might react with InSe for the formation of tetragonal  $\text{CuInSe}_2$ . The average grain sizes increased obviously with the increased temperatures. A possible reaction path to obtain a chalcopyrite structural film was discussed in the end. In addition, Ga was detected rich in the bottom of the film by energy dispersive spectroscopy and grazing incidence X-ray diffraction.

## 1 Introduction

Chalcopyrite semiconductors are promising materials for high efficiency and low cost thin film solar cells [1]. Copper indium gallium selenide (CIGS) based polycrystalline semiconductor is used for thin film solar cells, and is one of the most popular choices in the recent years [2, 3]. The efficiency of laboratory scale CIGS device has reached 20.3 % [4]. Different promising synthesis routes for CIGS absorber layers have been investigated [5–7]. A synthesis route is the deposition of metallic precursors onto a back electrode followed by evaporating Se and subsequent thermal processing. That process is used to fabricate high efficiency solar cells [8]. Knowledge of the phases involved in the chalcopyrite formation is essential for the development of an atomistic understanding of the growth process [9].

The grain growth in polycrystalline CIGS is important to the cell efficiency [10]. As widely believed, copper selenide formed during selenization can enhance grain growth of CIGS absorbers [11, 12]. A vapour-liquid–solid mechanism is used to explain the grain growth of CIGS [13]. First, the binary selenide phase like CuSe forms in the surface. Then, it can enhance in out-diffusion to the surface and react with Se. Finally, these two phases react upon annealing with the element Se to form  $\text{CuInSe}_2$ . The nature of intermediate phases formed during selenization is under discussion in some literatures [14–16]. Though copper selenide is a key phase for crystalline growth, it also results in the degradation of CIGS solar cells in Cu-rich condition since the presence of Cu–Se phases provides recombination sites for the minority charge carriers, reducing overall cell performance [17]. Therefore, Cu-poor CIGS film is required to fabricate highly efficient solar cells [18].

---

J. Han · C. Liao · T. Jiang · H. Xie  
Department of Physics, Peking University, Beijing 100871,  
China

J. Han (✉)  
Institut des Matériaux Jean Rouxel (IMN), Université de Nantes  
UMR CNRS 6502, 2 rue de la Houssinière, BP 32229,  
44322 Nantes Cedex 3, France  
e-mail: pkuhjf@gmail.com; junfeng.han@cnrs-imn.fr

C. Liao  
Chengdu Green Energy and Green Manufacturing Technology  
R and D Centre, Chengdu 601207, Sichuan Province, China

In this work, the aim was to investigate the evolution of film structures and morphologies during selenization. The metal precursors (CuGa, In) were deposited on top of a Mo coated soda-lime glass. The stacked elemental precursors were annealed in a selenium-contained atmosphere. Samples were submitted to selenization steps with temperature ranges from 210 to 380 °C. Thin films were analyzed by SEM, TEM, XRD and Raman spectra.

## 2 Experiment

### 2.1 Film growth

In the first step, the precursor (CuGa/In/CuGa/In) were deposited at room temperature by alternately DC magnetron sputtering of CuGa (75 % Cu + 25 % Ga) and In targets at a pure Argon pressure of 1 Pa. Thin films were deposited on Mo-coated  $7.5 \times 2.5 \text{ cm}^2$  soda-lime glass substrates. The thicknesses of CuGa and In films were 100 and 200 nm respectively (see Fig. 1). More experimental details concerning the precursors were given in references [19, 20].

The metallic precursors were put in a specially designed tube furnace, as shown in Fig. 1. The Ar pressure was maintained at 200 Pa during selenization. Excessive selenium platelets were placed around the samples to create a selenium over-pressure and thus compensate Se mass losses in the annealing process. The ramping rate of the furnace was set to 1 °C/s. Samples were submitted to a 30 min annealing at the following temperatures respectively: 210, 240, 270, 310, 340, 380 °C. These temperature values were selected in order to investigate the reaction processes involved in selenization.

### 2.2 Characterization

The surface morphologies of thin films were investigated by field emission scanning electron microscopy (FESEM). All samples were investigated using 10 kV beam (Nova nano SEM 430, 1.5 nm resolution). The compositions of thin films were analyzed by energy dispersive spectroscopy

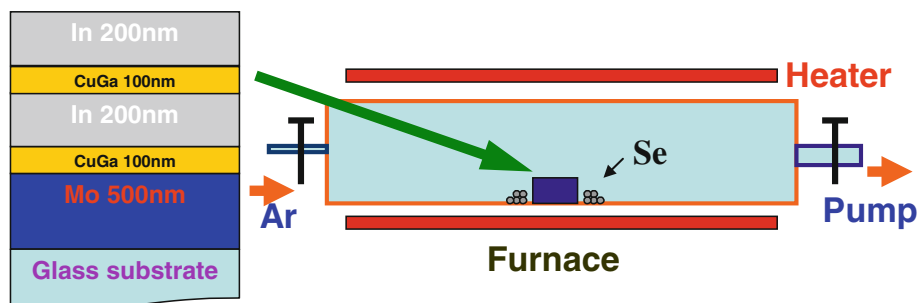
(EDS). Transmission electron microscopy (TEM) study was performed with Hitach HNAR 9000 microscope. Samples for TEM studies were prepared by scratching the surface of thin films and depositing the results onto a gold grid coated with holey-carbon film. The electron diffraction patterns were performed using the selected area electron diffraction mode. The crystalline phases were examined by X-ray diffraction (XRD) using RICOH-DX12 with Cu  $K\alpha$  ( $\lambda = 1.5418 \text{ \AA}$ ) radiation. All diffraction peaks were determined by comparison with JCPDS data files. The Raman spectra were recorded in back scattering geometry at room temperature, using a T64000 Jovin Yvon spectrometer with the He–Ne 633 nm laser line. The incident power was set by attenuating the laser beam with the use of neutral density filters. A 0.1 mW power for the laser point diameter of  $4 \mu\text{m}^2$  was used to get a detectable signal without destroying the samples. Related references were used to identify those Raman shifts [21–23].

## 3 Results

### 3.1 Morphological evolutions of the thin films in the annealing process

Figure 2a–g show typical SEM images of samples annealed at temperature range from 210 to 380 °C. Increased temperatures result in significant modification of thin film surface morphologies. At a low temperature of 210 °C (Fig. 2a), a great amount of thin platelets appear in the film surface. The average thicknesses of those platelets are less than 50 nm. The sizes of those platelets are more than 500 nm. Most platelets have hexagon or polygon structures. For an annealing temperature of 240 °C (Fig. 2b), more and more platelets appear in the film surfaces. The average sizes of these platelets increase to 1–2  $\mu\text{m}$ , and average thicknesses are more than 100 nm. Then, at 270 °C (Fig. 2c), the sizes of those platelets are maintained the same values. They have more regular shapes and sharper edges. While increasing annealing temperature up to 310 °C (Fig. 2d), most platelets cannot be observed by SEM. Only a few large platelets are seen in

**Fig. 1** The annealing system: Se platelets were placed around the metal precursors. Ar flew through the tube and was pumped out during selenization



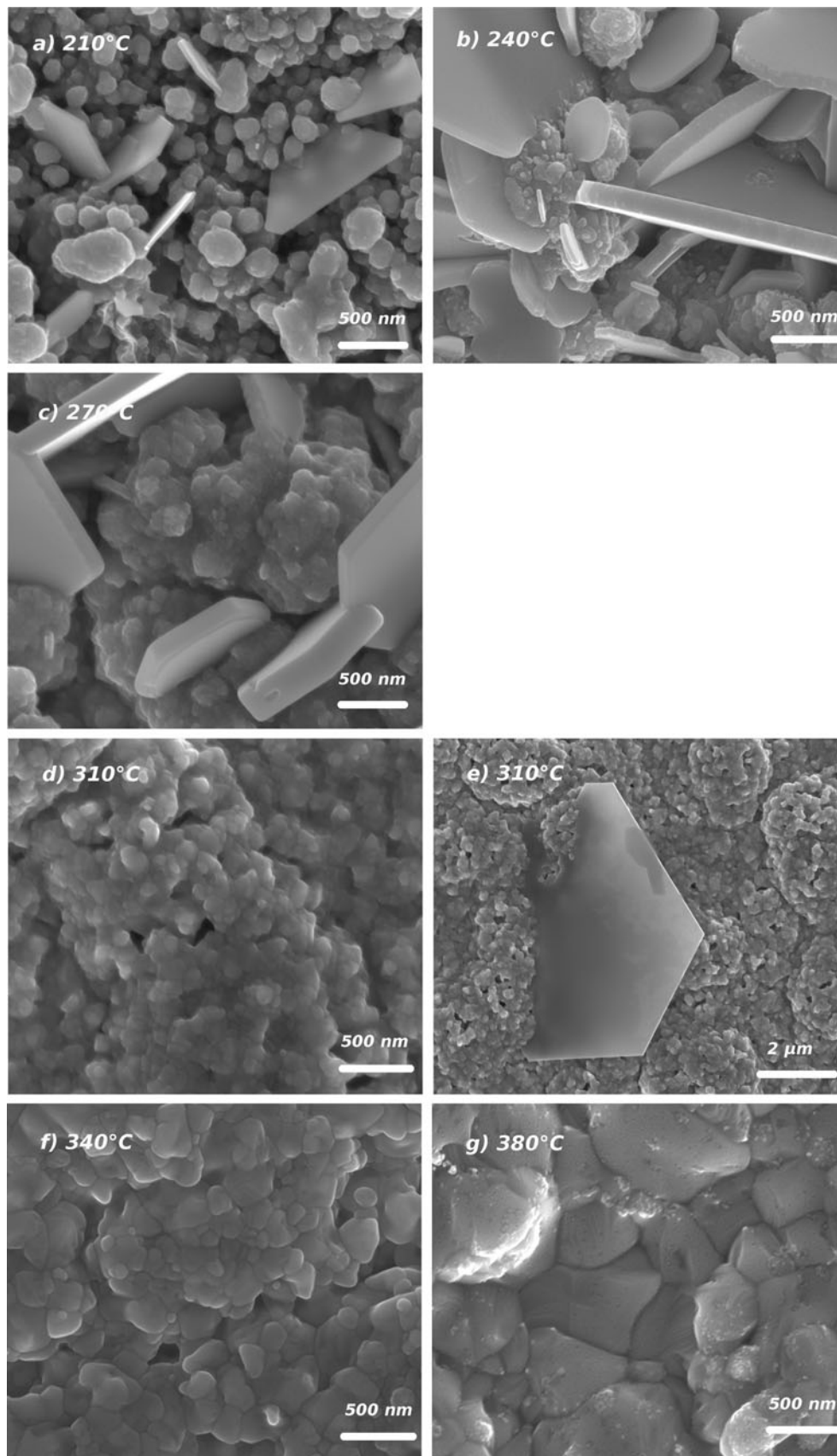
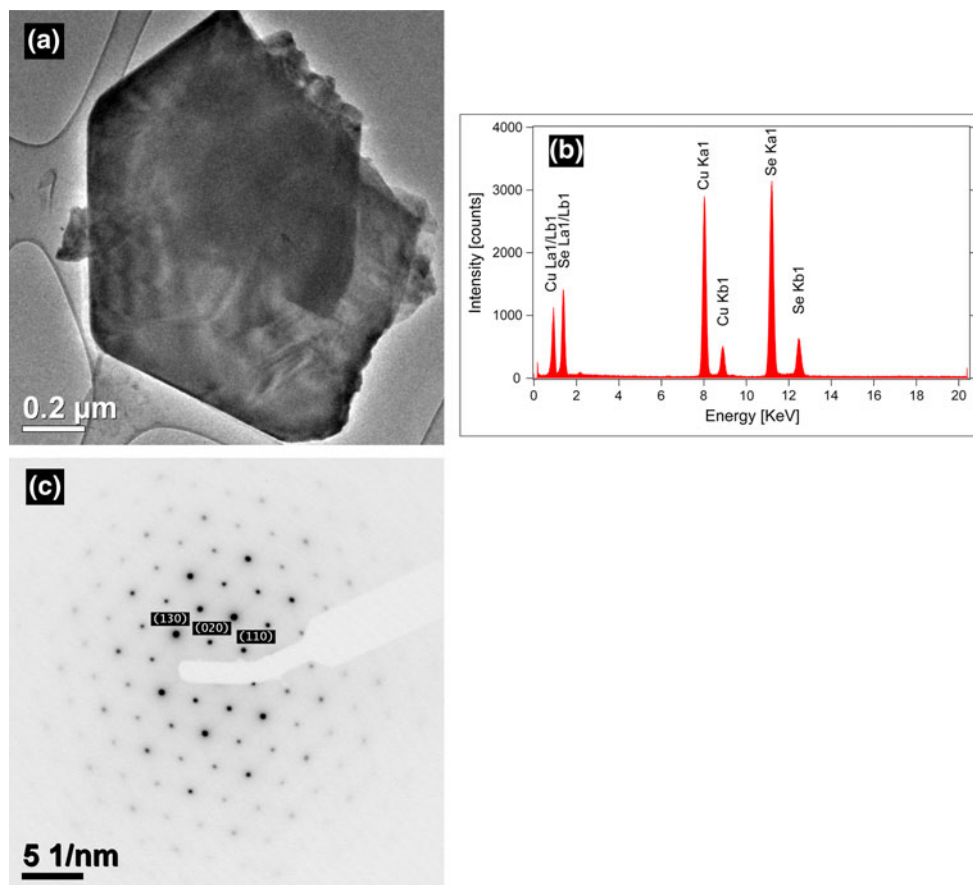


**Fig. 2** SEM images of samples selenized at temperature range from 210 to 380 °C

**Fig. 3** TEM analyses of CuSe platlets scratched from samples selenized at 240 °C: **a** TEM images of the platlets; **b** EDS analyses on the platlets; **c** electron diffraction patterns from selected area on the platelets



the low-magnification-mode image as shown in Fig. 2e. Finally, when the annealing temperature is reaching 340 °C (Fig. 2f), no platelet is observed any more in the film surface.

To investigate the structures and components of those platelets, films are scratched from the substrates and analyzed by TEM. Some isolated platelets are observed under the microscopy. Figure 3a shows a typical image of the isolated platelet on the TEM sample grid. It has a polygon structure. That platelet is also analyzed by EDS as shown in Fig. 3b. Cu and Se signals are detected, while In and Ga signals do not exist in the spectrum. Quantity calculations from EDS spectra indicate that the atomic ratio of Cu and Se is nearly 1:1. Furthermore, from electron diffraction pattern (Fig. 3c), these platelets consist of the  $\gamma$ -CuSe phase (PCPDF file n 27-0185).

In the SEM images, below 310 °C, backgrounds of the thin films are composed of small grains with the sizes of 50–100 nm and no obvious increase of grain sizes can be observed. Then, at 340 °C (Fig. 2f), the average grain sizes have a slight increase to around 200 nm. When the temperature reaches 380 °C, the average grain sizes become more than 500 nm as shown in Fig. 2g. The film seems to be more compact. An EDS analysis is used to investigate the atomic ratio of thin film from the plane view: the

metallic precursors are composed of 42 % Cu, 12 % Ga and 45 % In while the selenized films contain 22 % Cu and 26 % In and 52 % Se. It is a Cu-poor chalcopyrite film.

Ga is detected in the precursor layer. However, after selenization, no Ga component can be detected in the film surface. To investigate the Ga location, the sample selenized at 380 °C was peeled off from substrate and analyzed by EDS. The results indicated that the bottom part were composed of 22 % Cu, 10 % Ga, 20 % In and 48 % Se. Therefore, we can conclude that Ga is rich in the bottom part of the thin film but poor in the surface.

### 3.2 XRD patterns of the thin films in the annealing process

In order to investigate the different crystallization steps involved during selenization, the precursors were annealed at temperatures range from 210 to 380 °C. Corresponding XRD patterns are displayed in Fig. 4. Two peaks at 40.4° and 87.4° observed in all patterns correspond to Mo film substrate.

Starting from the bottom of Fig. 4, at 210 °C, five diffraction peaks are observed, lying at 30.0°, 32.9°, 36.6°, 39.1° and 42.9°. Two peaks at 30.0° and 32.9° are respectively associated to the diffraction planes 101 and

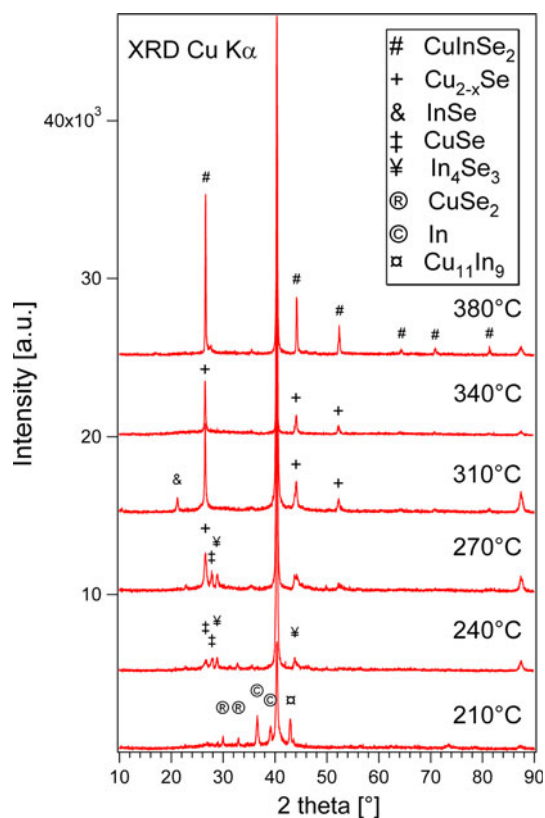


**Fig. 4** XRD patterns of samples selenized at temperature range from 210 to 380 °C

111 of  $\text{CuSe}_2$  (PDF-00-026-1115- $\text{CuSe}_2$ ). Two other diffraction peaks at  $36.6^\circ$  and  $39.1^\circ$  are related with 002 and 110 planes of metallic In crystalline (PDF-01-085-1409-In). The peak at  $42.9^\circ$  belongs to  $\text{Cu}_{11}\text{In}_9$  (PDF-00-041-0883- $\text{Cu}_{11}\text{In}_9$ ). Then, with increased temperature to 240 °C, the intensity of the peak at  $32.9^\circ$  has an obvious decrease, while four new diffraction peaks are observed at  $26.6^\circ$ ,  $27.9^\circ$ ,  $28.8^\circ$  and  $43.8^\circ$ . The peaks at  $26.6^\circ$  and  $27.9^\circ$  are respectively associated to the diffraction plane 101 and 102 of  $\text{CuSe}$  (PDF-00-049-1457- $\text{CuSe}$ ). Two other peaks at  $28.8^\circ$  and  $43.8^\circ$  might be related respectively with 040 and 002 of  $\text{In}_4\text{Se}_3$  phases (PDF-00-048-1575- $\text{In}_4\text{Se}_3$ ). Thus, increased temperature results in the decomposition of  $\text{CuSe}_2$  and the synthesis of In-Se compounds simultaneously. At 270 °C, intensity of the peak at  $26.6^\circ$  has an obvious increase and simultaneously the peak at  $43.8^\circ$  extends broader. This may be caused by a formation of  $\text{Cu}_{2-x}\text{Se}$  phase. The related diffraction angles of  $26.6^\circ$  and  $44.1^\circ$  correspond to 111 and 220 planes of  $\text{Cu}_{2-x}\text{Se}$  phase (PDF-01-071-0044- $\text{Cu}_{2-x}\text{Se}$ ). Then, with further increasing temperature up to 310 °C, the peaks at  $27.9^\circ$  and  $28.8^\circ$  are disappeared, while two other peaks lying at  $21.2^\circ$  and  $52.3^\circ$  are observed in the patterns. The peak at  $43.8^\circ$  has a slight shift to the right direction. Compared with references from JSPDS cards, the peak at  $21.2^\circ$  corresponds to 006

diffraction plane of InSe phase (PDF-00-044-1007-InSe), and three other peaks belong to  $\text{Cu}_{2-x}\text{Se}$  phase. The selenization beyond 310 °C leads to a complete decomposition of  $\text{CuSe}$  and  $\text{In}_4\text{Se}_3$ , and consequently formation of InSe and  $\text{Cu}_{2-x}\text{Se}$  phases in the film. When the temperature is reaching 340 °C, the diffraction peaks of InSe phase turn to be disappeared and simultaneously the intensities of peaks at  $26.6^\circ$ ,  $44.1^\circ$  and  $52.3^\circ$  have obviously decreased. Finally, at 380 °C, the pattern is composed of six diffraction peaks, lying respectively at  $26.6^\circ$ ,  $44.2^\circ$ ,  $52.4^\circ$ ,  $64.3^\circ$ ,  $70.9^\circ$  and  $81.3^\circ$ . All of these peaks indicate a typical chalcopyrite structure of  $\text{CuInSe}_2$  phase forming in the film (PDF-01-081-1936- $\text{CuInSe}_2$ ). The intensities of the three main peaks at  $26.6^\circ$ ,  $44.2^\circ$  and  $52.4^\circ$  increase with reduced full width half maximum values.

Though there is a amount of Ga in the precursor, Ga related phases are not detected by XRD technology throughout the annealing process from 210 to 380 °C. To investigate Ga related phases in the film, the sample selenized at 380 °C was peeled off from substrate. The top and bottom layers of the thin films were both analyzed by grazing incidence X-ray diffraction (GIXRD). The incidence angle was set to  $1^\circ$  to get the enough signal intensities. The detection depth by using this angle was 100–200 nm. Figure 5 shows the GIXRD patterns of top and bottom parts of the thin films. The pattern from top layer consists of three diffraction peaks, lying respectively at  $26.6^\circ$ ,  $44.2^\circ$ ,  $52.4^\circ$ , which indicates a typical chalcopyrite structure of  $\text{CuInSe}_2$  phase. The pattern from bottom layer shows that the 112 peak shifts to  $26.9^\circ$ , with an obvious shoulder on the right sides. It indicates possible Ga-rich phases at the bottom layer. The results have a good agreement with EDS analyses. The position of the 112 diffraction peak of CIS is close to  $26.6^\circ$ , while that of CGS is at a higher angle ( $27.7^\circ$ ). The diffraction peak shift is caused by the reduction in the lattice parameters because In atoms are substituted by the smaller Ga atoms.

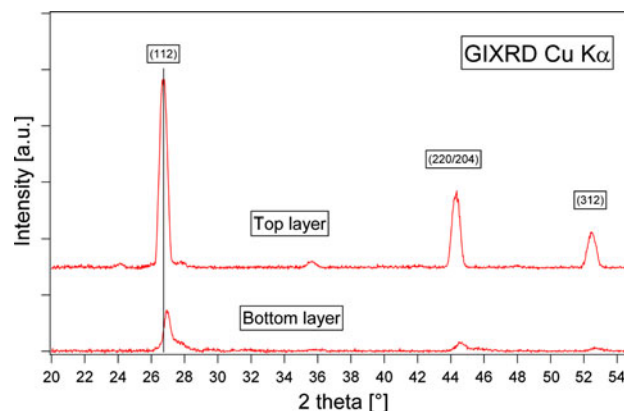


**Fig. 5** GIXRD patterns from *top* and *bottom* parts of the thin film selenized at 380 °C

### 3.3 Raman spectra of the thin films in the annealing process

Figure 6 depicts micro-Raman spectra of absorber films measured at room temperature. Related references are used to identify those Raman shifts [21–23]. Starting from the top of Fig. 6, at 210 °C, a frequency of A1 mode of Cu–Se compound, such as CuSe, CuSe<sub>2</sub>, is seen at 260 cm<sup>-1</sup> from the spectrum. In addition, a broad mode at 185 cm<sup>-1</sup> seems to be related to Cu–Se compound. The broad peaks at 147 and 243 cm<sup>-1</sup> may indicate the existence of a metastable multi-phase in relation to polycrystalline In–Se compound. At 240 °C, intensities of the Cu–Se A1 mode and the In–Se compound increase obviously. An additional peak at around 200 cm<sup>-1</sup> may also relate with In–Se compound. With further increasing temperature up to 270 °C, the peaks of Cu–Se compounds become more strong and narrow, while intensities of In–Se peaks decrease a lot. Several weak peaks are observed in the spectra, lying at 174, 212 and 228 cm<sup>-1</sup>. They may be associated to CuInSe<sub>2</sub> A1 mode, E mode and B2 mode respectively. Further selenization at 310 °C results in serious decrease of peak intensity of Cu–Se A1 mode. That peak exists in the spectra till

340 °C. Finally, at 380 °C, the spectrum is composed of three peaks lying at 174, 212 and 228 cm<sup>-1</sup>, which are respectively associated to CuInSe<sub>2</sub> A1, E and B1 modes. A single chalcopyrite CuInSe<sub>2</sub> phase forms in the film surface.

### 4 Discussion

With the annealing temperature from 210 to 270 °C, CuSe<sub>2</sub>, CuSe and In<sub>4</sub>Se<sub>3</sub>, were detected in the films by XRD. A large number of platelets were observed clearly in the SEM images. Those platelets grew up with the increased temperature from 210 to 270 °C. Then, they were disappeared beyond 310 °C. TEM analyses indicated that these platelets corresponded to the γ-CuSe phase, which was also observed by another group in their electric-deposited films [24]. XRD patterns and Raman spectra also confirmed the existence of CuSe phase from 240 to 310 °C. Above 310 °C, Cu<sub>2-x</sub>Se and InSe phases became clearly in the film and contributed to the formation of CuInSe<sub>2</sub> phase. Therefore, a possible reaction path for CuInSe<sub>2</sub> phase formation is assumed as the following equations:



CuSe<sub>2</sub> was not very stable and decomposed very quickly with the increased temperatures. CuSe could react with InSe to form CuInSe<sub>2</sub>, which was a possible reaction path as mentioned in some other references [14, 15]. However, in our case, due to a complete decomposition of CuSe below 340 °C, reaction between Cu<sub>2-x</sub>Se and InSe seemed to be a more possible path to form CuInSe<sub>2</sub> compounds. A complete reaction of CuInSe<sub>2</sub> phase formation was finished at 380 °C and the grain sizes increased from 200 to 500 nm.

Ga was accumulated at the bottom of the films. That was mainly caused by the different out-diffusion of Ga and In during selenization [25]. First, copper selenide formed in the surfaces of thin films. Then, Ga and In diffused out to the surfaces and reacted with copper selenide. Because In had a larger atomic radius than Ga, the strain energy of the film was lower by preferential out-diffusion of In relative to Ga. The indium reacted with Cu and Se delivered to the films to form new unit cells in the surfaces, which contributed to a growth in the film thickness. In this way, the additional film thickness became Ga depleted relative to the film back.

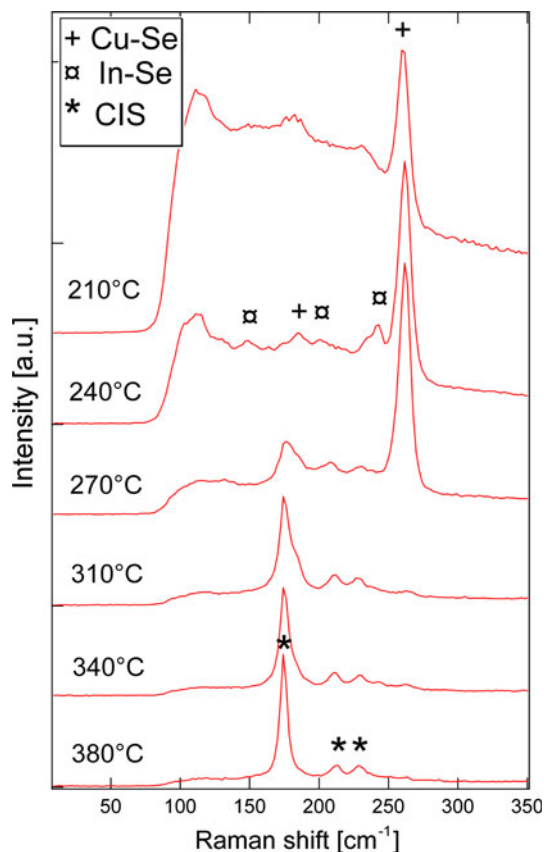


Fig. 6 Raman spectra of samples selenized at temperature range from 210 to 380 °C

## 5 Conclusion

In this work, selenization was studied to understand the evolution of the Cu-In-Ga-Se system. Metallic precursors selenided at temperature range from 210 to 380 °C were investigated by SEM, TEM, XRD and Raman. A large number of CuSe platelets were seen clearly from 210 to 270 °C. Above 310 °C, most of CuSe platelets decomposed under release of selenium and formed  $\text{Cu}_{2-x}\text{Se}$ . Finally,  $\text{Cu}_{2-x}\text{Se}$  reacted with InSe to form  $\text{CuInSe}_2$ , and the grain sizes increased from 200 to 500 nm. Ga was accumulated at the bottom of the selenized film.

**Acknowledgments** The authors want to thank Zhang Hui-zhen for sample preparation and analysis by FESEM. The presented results were supported by the Beijing Ministerium for the science project under contract no.H030630010120.

## References

1. T. Nakada, *Electron. Mater. Lett.* **8**, 179 (2012)
2. J. Kaneshiro, N. Gaillard et al., *Sol. Energy Mater. Sol. Cells* **94**, 12 (2010)
3. S.Y. Kim, J.H. Kim, *J. Korean Phys. Soc.* **60**, 2018 (2012)
4. P. Jackson, D. Hariskos et al., *Prog. Photovolt Res. Appl.* **19**, 894 (2011)
5. T.J. Gillespie, C.H. Marshall, *Sol. Energy Mater. Sol. Cells* **59**, 27 (1999)
6. C.J. Hibberd, E. Chassaing et al., *Prog. Photovolt Res. Appl.* **18**, 434 (2010)
7. C.H. Shen, Y.C. Lin, *J. Mater. Sci. Mater. Electron.* **24**, 2906 (2013)
8. J.K. Sim, K. Ashok et al., *Met. Mater. Int.* **19**, 303 (2013)
9. F.B. Dejene, *Curr. Appl. Phys.* **10**, 36 (2010)
10. S. Niki, M. Contreras et al., *Prog. Photovolt Res. Appl.* **18**, 453 (2010)
11. D. Wolf, G. MuÈller, *Thin Solid Films* **361–362**, 155 (2000)
12. S. Ishizuka, H. Shibata et al., *Appl. Phys. Lett.* **91**, 041902 (2007)
13. R. Klenk, T. Walter et al., *Adv. Mater.* **5**, 114 (1993)
14. J. Liu, A.X. Wei et al., *J. Mater. Sci. Mater. Electron.* **24**, 2553 (2013)
15. N.H. Kim, S. Oh et al., *J. Korean Phys. Soc.* **61**, 1177 (2012)
16. F. Hergert, S. Jost et al., *Part. Part. Syst. Character.* **22**, 423 (2005)
17. S. Han, F. Hasoon et al., *J. Phys. Chem. Solids* **66**, 1895 (2005)
18. T.P. Hsieh, C.C. Chuang et al., *Solid-State Electron.* **56**, 175 (2011)
19. C. Liao, J. Han, K. Zhao et al., *Chin. J. Inorg. Chem.* **27**, 1 (2011)
20. C. Liao, J. Han, K. Zhao et al., *Acta Phys. Chim. Sin.* **27**, 432 (2011)
21. W. Witte, R. Kniese et al., *Thin Solid Films* **517**, 867 (2008)
22. K.H. Liao, C.Y. Sua et al., *Appl. Surf. Sci.* **263**, 476 (2012)
23. T. Mise, T. Nakada, *Sol. Energy Mater. Sol. Cells* **93**, 1000 (2009)
24. A. Gobeaut, L. Laffont, J.M. Tarascon et al., *Thin Solid Films* **517**, 4436 (2009)
25. S. Schleussner, U. Zimmermann et al., *Sol. Energy Mater. Sol. Cells* **95**, 721 (2011)